APPLIED GEOPHYSICS, Vol.9, No.3 (September 2012), P. 326 - 332, 4 Figures.
DOI: 10.1007/s11770-012-0340-6

Seismic low-frequency-based calculation of reservoir fluid mobility and its applications*

Chen Xue-Hua[1,2], He Zhen-Hua[1,2], Zhu Si-Xin[3], Liu Wei[2], and Zhong Wen-Li[4]

Abstract: Low frequency content of seismic signals contains information related to the reservoir fluid mobility. Based on the asymptotic analysis theory of frequency-dependent reflectivity from a fluid-saturated poroelastic medium, we derive the computational implementation of reservoir fluid mobility and present the determination of optimal frequency in the implementation. We then calculate the reservoir fluid mobility using the optimal frequency instantaneous spectra at the low-frequency end of the seismic spectrum. The methodology is applied to synthetic seismic data from a permeable gas-bearing reservoir model and real land and marine seismic data. The results demonstrate that the fluid mobility shows excellent quality in imaging the gas reservoirs. It is feasible to detect the location and spatial distribution of gas reservoirs and reduce the non-uniqueness and uncertainty in fluid identification.
Keywords: fluid mobility, seismic low-frequency, reservoir characterization, fluid identification, instantaneous spectral decomposition

Introduction

The low-frequency components of reflected seismic waves are extremely important in reservoir exploration. Recently, there are increasingly excellent advances and successful examples in characterizing reservoir features and detecting hydrocarbons by exploiting the low-frequency behavior of seismic response. The main indicators of reservoirs from seismic low-frequencies include low-frequency shadows associated with hydrocarbon deposits (Sun et al., 2002; Castagna et al., 2003; Chen et al., 2009), low-frequency energy anomalies (Goloshubin et al., 2002; Goloshubin et al., 2006; Korneev et al., 2004), and instantaneous wavelet energy absorption analysis in the low-frequency domain (Lichman and Goloshubin, 2003; Lichman et al., 2004a, 2004b). The induction mechanisms of the low-frequency components-based hydrocarbon indications are investigated by using both rock physics and numerical modeling (Liu, 2004; Batzle et al., 2006; Ebrom, 2004; He et al., 2008; Chen et al., 2009; Chen et al., 2011;

Manuscript received by the Editor April 18, 2012; revised manuscript received July 4, 2012.
*This work was supported by the National Natural Science Foundation of China (No. 41004054), the National Science and Technology Major Project of the Ministry of Science and Technology of China (No. 2011ZX05023-005-010), the Research Fund for the Doctoral Program of Higher Education of China (No. 20105122120002).
1. State Key Laboratory of Oil and Gas Reservoir Geology and Exploitation, Chengdu University of Technology, Chengdu 610059, China Email: chen_xuehua@163.com.
2. Key Laboratory of Earth Exploration and Information Technology of Ministry of Education, Chengdu University of Technology, Chengdu 610059, China.
3. North China University of Water Resources and Electric Power, Zhengzhou 450011, China.
4. College of Earth Sciences, Chengdu University of Technology, Chengdu 610059, China.

Quintal et al., 2007; Tai et al., 2009). Such methods and works enhance the reliability of reservoir imaging and hydrocarbon detection and demonstrate the importance of seismic low-frequency exploitation. However, these hydrocarbon indications show no direct relationships with reservoir fluid mobility measurements. Silin et al. (2004) have obtained an asymptotic representation of the seismic reflection from a fluid-saturated porous medium in the low-frequency domain. They derived the equations of low-frequency harmonic waves in a fluid-saturated elastic porous medium from the basic concepts of filtration theory. It turned out that these equations can be related to the Frenkel-Gassmann-Biot poroelasticity model and to the pressure diffusion model routinely used in well test analysis as well. They defined a dimensionless small parameter from fluid mobility and diffusion mechanisms and obtained an asymptotic representation of the frequency-dependent reflection coefficient of the fluid-saturated reservoir. It turned out that the frequency-dependent reflection coefficient in the low-frequency domain is proportional to the square root of the product of the fluid mobility (defined as permeability to viscosity ratio) in the reservoir, the fluid density, and the seismic signal frequency. A reservoir imaging attribute derived from this theory has been applied to predict the location of the oil-water contact and measure reservoir production rate (Goloshubin et al., 2006; Korneev et al., 2005; Goloshubin et al., 2008). This theory can be expected to provide a feasible method for predicting gas reservoir properties in absence of well data (Hilterman et al., 2007).

We derive a computational implementation of reservoir fluid mobility measurement from the theory of Silin et al. (2004) and present the optimal frequency determination in the low-frequency domain in this paper. Furthermore, the direct calculation methods of the fluid mobility measurements using the time-frequency spectra at the optimal frequency in the low-frequency domain are implemented. The methods are then applied to both land and marine seismic data and the results show well correlated imaging with the known gas reservoirs.

Theory and methods

Theory of reservoir fluid mobility

Silin et al. (2004) performed the low-frequency asymptotic analysis of seismic reflections from the interface between elastic and elastic fluid-saturated porous media. They first derived the wave equations in elastic fluid-saturated porous media from filtration theory, which modifies Darcy's law in order to adopt inertial and non-equilibrium effects. Then the equations were proved relating to the Frenkel-Gassmann-Biot poroelasticity model and the pressure diffusion model routinely used in well test analysis. The equations take into account the combination of filtration theory and poroelasticity principles (Silin et al., 2004). In addition, they presented a harmonic wave solution to the equations derived from filtration theory and introduced the dimensionless small parameters for the asymptotic analysis. Then the asymptotic representation of the seismic reflection from a fluid-saturated porous medium in the low-frequency domain was established.

Considering the seismic reflection from the interface between elastic and fluid-saturated porous media, within a reasonable range of rock and fluid properties, the dimensionless parameter $\varepsilon = i\frac{\kappa\rho_f}{\eta}\omega$ is small at low (below 1 KHz) frequencies (Silin et al., 2004; Korneev et al., 2005; Silin and Goloshubin, 2008, 2009). The frequency-dependent coefficient R of a planar compression wave at angular frequency ω from the interface has the form:

$$R = R_0 + R_1(1+i)\sqrt{\frac{\kappa\rho_f}{\eta}\omega}, \tag{1}$$

where R_0 and R_1 are real coefficients which are functions of the mechanical properties (including porosity, density, and elastic coefficients) of the reservoir rock and fluid, $i = \sqrt{-1}$, κ denotes the reservoir permeability, η is the fluid viscosity, and ρ_f is the reservoir rock bulk density. The absolute value of the low-frequency reflection coefficient attains its maximum at $\frac{\omega\kappa}{\eta} = 0$ (i.e. $\varepsilon = 0$).

Assuming that the reservoir fluid mobility $\mathbf{F} = \frac{\kappa}{\eta}$, which is defined as the reservoir permeability to the fluid viscosity ratio, it is evident in equation (1) that the seismic reflection coefficients are related closely to the fluid density, the seismic signal frequency, and the reservoir fluid mobility. To extract the fluid mobility measurement from the seismic data, the deriving equations are given in this paper below.

Taking the derivative of equation (1) with respect to frequency, we obtain

$$\frac{dR}{d\omega} = \frac{R_1(1+i)}{2}\sqrt{\frac{\rho_f}{\omega}}\sqrt{\frac{\kappa}{\eta}}. \tag{2}$$

Let us put $\mathbf{C} = \frac{R_1(1+i)}{2}\sqrt{\rho_f}$, which is a complex function of the elastic properties of the porous fluid and rock matrix. Then the following equation is true:

$$\frac{dR}{d\omega} = \mathbf{C}\omega^{-\frac{1}{2}}(\kappa/\eta)^{\frac{1}{2}} = \mathbf{C}\omega^{-\frac{1}{2}}\mathbf{F}^{\frac{1}{2}}. \tag{3}$$

Thus, the reservoir fluid mobility $\mathbf{F}_Z$ can be expressed as

$$\mathbf{F} = \frac{\kappa}{\eta} = \frac{1}{\mathbf{C}^2}\left(\frac{dR}{d\omega}\right)^2 \omega. \tag{4}$$

Equation (4) implies that the reservoir fluid mobility is proportional to the first derivative of the reflection coefficient at frequency ω. The instantaneous spectral amplitude or energy with respect to a common frequency after time-frequency decomposition of the seismic signal can truly indicate the energy or amplitude of the seismic reflection at this frequency. Thus, by substituting the instantaneous spectral amplitude $a(\omega)$ for the reflection coefficient R at frequency ω in real implementation, we obtain

$$\mathbf{F} \approx \frac{1}{\mathbf{C}^2}\left[\frac{\partial a(\omega)}{\partial \omega}\right]^2 \omega. \tag{5}$$

Due to the excellent time-frequency localization of the generalized S transform (Chen et al., 2009), this property can reduce the implementation distortion resulting from the thin-bed tuning effect. Thus, $a(\omega)$ in equation (5) can be calculated from the instantaneous spectra of the seismic signal using the generalized S transform. To implement equation (5), we need to first determine the frequency ω in the seismic low-frequency domain and then the coefficient $\mathbf{C}$. The parameters determination is described in the following sections.

Parameter determination in the reservoir fluid mobility calculation

Silin and Goloshubin (2010) derived a theoretical expression for the frequency-dependent compression reflection from a permeable layer. The reflection coefficient was defined as a function of a dimensionless parameter ε and it attains peak value in the low-frequency end of the spectrum. We introduce this theory to determine the optimal frequency in the implementation of the reservoir fluid mobility. We define the dimensionless parameter ε-dependent reflection factor given by

$$\psi(|\varepsilon|) = \sqrt{|\varepsilon|}e^{-\frac{\eta}{\kappa}\sqrt{\frac{\gamma_\beta+\gamma_k^2}{2M\rho_f}}\sqrt{|\varepsilon|}H}, \tag{6}$$

where $M = K + \frac{4}{3}\mu$ and H denotes the reservoir thickness. The dimensionless coefficients γ_K and γ_β are defined as

$$\gamma_\beta = K\left(\beta_f\phi + \frac{1-\phi}{K_{fg}}\right),\ \gamma_k = 1 - \frac{(1-\phi)K}{K_{sg}}, \tag{7}$$

where ϕ is the porosity and K is the dry rock bulk modulus. The other two elastic moduli are defined by

$$K_{sg} = \frac{K_g}{1-\phi},\ K_{fg} = \frac{K_g}{1-K/K_g}. \tag{8}$$

Here, β_f in equation (7) is the coefficient of fluid adiabatic compressibility. Its relation with the bulk modulus K_f of the fluid is $\beta_f = \frac{1}{K_f}$. K_g is the bulk modulus of the rock matrix.

Equation (6) attains a maximum value of

$$\psi_{\max} = \frac{1}{H}\frac{\kappa}{\eta}\sqrt{\frac{2M\rho_f}{\gamma\beta+\gamma K^2}}e^{-1} \tag{9}$$

at the dimensionless coefficient

$$\sqrt{|\varepsilon|_{\max}} = \frac{1}{H}\frac{\kappa}{\eta}\sqrt{\frac{2M\rho_f}{\gamma\beta+\gamma K^2}} \tag{10}$$

and the corresponding frequency

$$f_{peak} = \frac{\kappa}{2\pi\eta H^2}\frac{2M}{\gamma\beta+\gamma K^2}. \tag{11}$$

Equation (11) can be used as a theoretical method for the optimal frequency determination in reservoir fluid mobility calculation. For example, if $M = 2\times10^{10}$Pa, $\gamma\beta + \gamma K^2 \approx 2.5$, $\kappa = 1$ Darcy, $\eta = 10^{-5}$ Pas, and $H = 5$ m, then the reflection factor $\psi(|\varepsilon|)$ calculated according to equation (6) is shown in Figure 1. It attains a peak value at $f_{peak} \approx 10$ Hz. We use this frequency as the optimal frequency in reservoir fluid mobility calculations. Thus, equations (6) and (11) can be regarded as reference equations for the optimal frequency determination.

After determining the optimal frequency, to determine the parameter $\mathbf{C}$, suppose we are given the optimal frequency ω_o ($\omega_o = 2\pi f_{peak}$) and let us put $\frac{\partial a(\omega)}{\partial \omega} = \mathbf{I}$.

Hence, equation (5) can be rewritten as

$$\mathbf{F} \approx \frac{\omega_o}{\mathbf{C}^2}\mathbf{I}^2. \tag{12}$$

We see in equation (12) that the reservoir fluid mobility is in the form of a parabolic function. Thus, assuming that the well production rate or the permeability properties are known, one can obtain the coefficient **C** from a parabolic fit of $\omega_o\mathbf{I}^2$ calculated at the known wells.

The coefficient **C** is equivalent to a proportional factor in equation (12). Thus, under conditions of no or few wells in the exploration area, one can directly calculate $\omega_o\mathbf{I}^2$ and obtain the relative reservoir fluid mobility measurement values in the absence of well data.

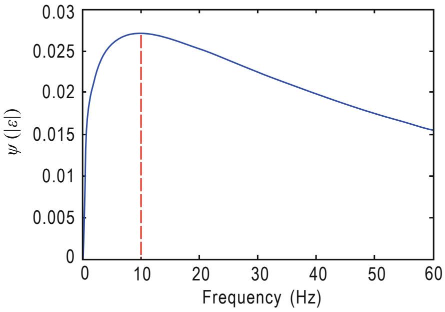

Fig. 1 P-wave frequency-dependent reflecting factor from a permeable layer.

Synthetic data example

To investigate the fluid mobility properties of the permeable reservoir, we design an anticlinal gas-bearing permeable reservoir model shown in Figure 2a. The layer shown in red denotes a highly permeable gas-bearing reservoir (indicated by a yellow arrow) and the dry layers are shown in gray. We obtain the synthetic seismic data (shown in Figure 2b) using a diffusive and viscous wave equation-based numerical simulation of the seismic response in the fluid-bearing poroelastic media (Chen et al., 2009; 2011; 2012). This wave equation takes into account the diffusive property of the fluid-bearing porous media and the viscosity of the fluid. As shown in Figure 2b, the seismic reflections of the permeable gas-bearing reservoir suffer from noticeable time delay and phase distortion. In Figure 2c, the permeable gas-bearing reservoir causes evident anomalies of the fluid mobility measurement.

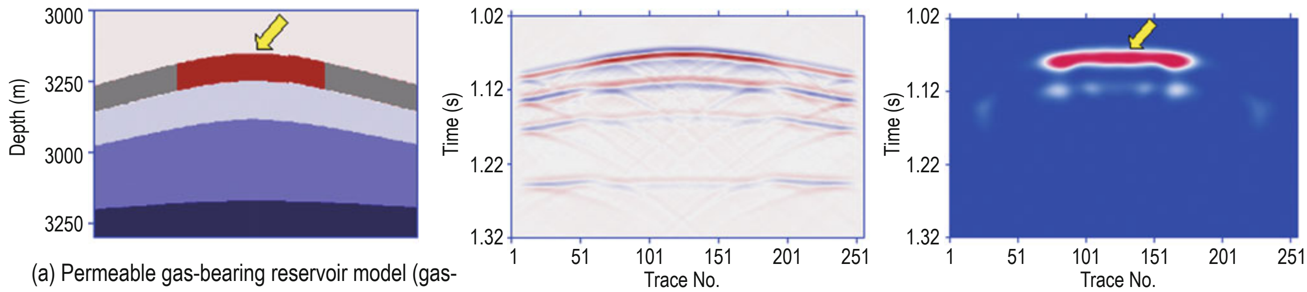

(a) Permeable gas-bearing reservoir model (gas-bearing layer is indicated by a yellow arrow)

(b) Synthetic seismic profile of the model

(c) Fluid mobility section of the model

Fig. 2 Fluid mobility analysis of the synthetic seismic data from a permeable gas-bearing reservoir model.

Real data applications

Our methodology and algorithm are applied to both land and marine 3D seismic data. The land seismic data is from the TH field, located in the Tarim Basin in Northwest China. There are Triassic braided streams and sandstone reservoirs distributed within channel deposits in this area. In Figure 3a, the top and bottom of the condensate gas reservoirs (indicated by a yellow arrow) are indicated on the well trajectory on the raw seismic section passing through well NH-1. The thickness of the reservoir is approximately 10 m and the mean porosity is 23.9%. The target reservoir strata show strong bright spot anomalies (indicated by the yellow arrow) on the reservoir fluid mobility section (Figure 3b). On the target horizon slice of the reservoir fluid mobility (Figure 3d), the spatial distribution and evident edge of the Triassic braided stream sandstone reservoir are all clearly delineated (indicated by the yellow arrow). The fluid mobility measurement is correlated well with the known production.

The marine seismic data is from the JZ area of the Bohai Sea, China. Prodelta and turbidite reservoirs are distributed in the target interval of E3d2L. The southwest-to-northeast big faults and some small faults are distributed at the target horizon. There is only one well J-2 with pay and the highest production rate at the horizon. In Figure 4a, the gas, oil, and water layers (marked by the well log on the zoom map) are indicated on the

Low-frequency-base reservoir fluid mobility

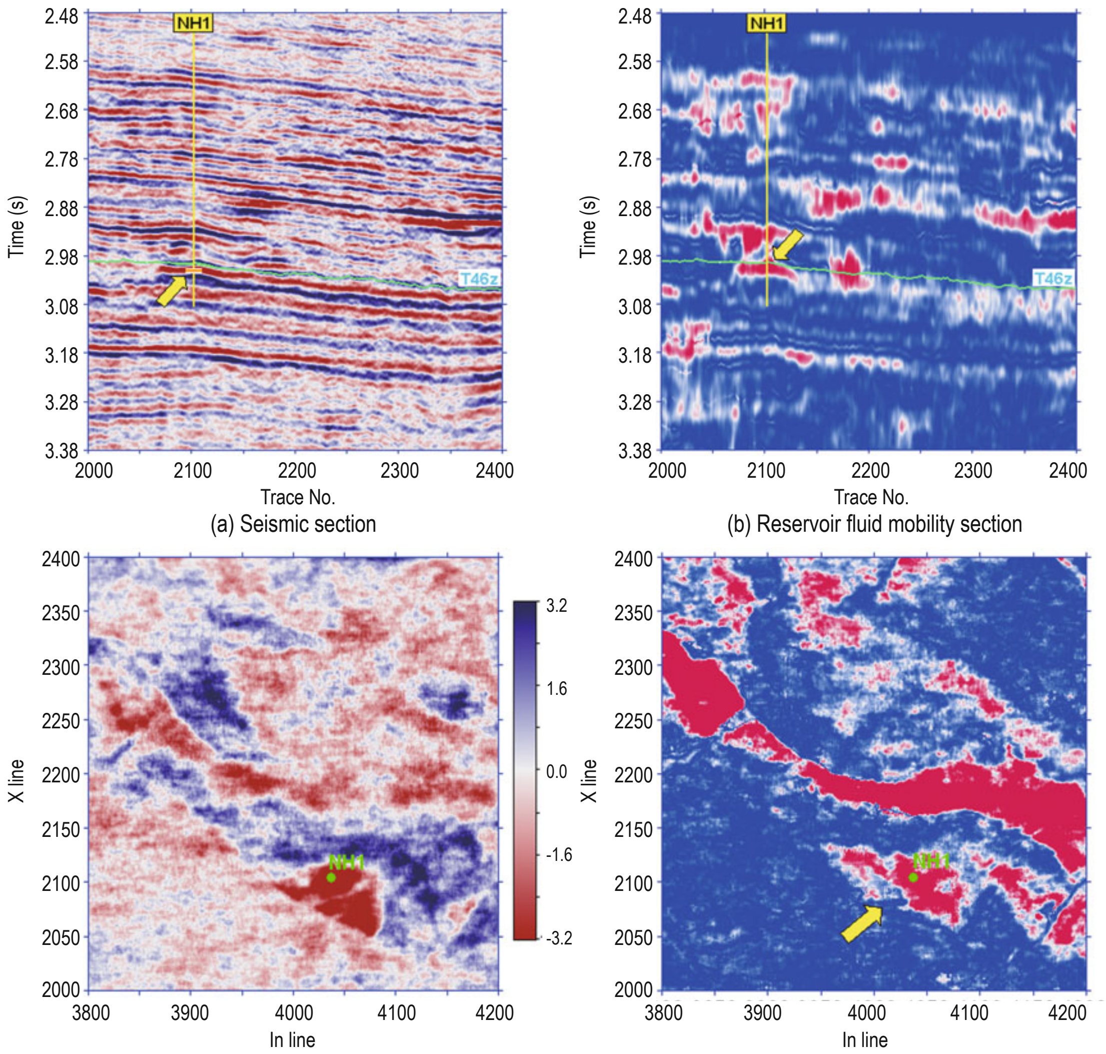

(a) Seismic section (b) Reservoir fluid mobility section

(c) Seismic slice (d) Reservoir fluid mobility slice.

Fig. 3 Fluid mobility analysis of reservoirs from TH area.

well trajectory on the raw seismic section passing through well J-2. The reservoir fluid mobility measurements in Figure 4b show a strong bright spot at the location of the gas reservoirs. The fluid mobility slice extracted along the gas reservoirs (Figure 4d) clearly delineates the spatial distribution, geometry, and evident edge of the gas reservoir (outlined by a black dashed contour). The gas reservoir correlates quite well with the known production.

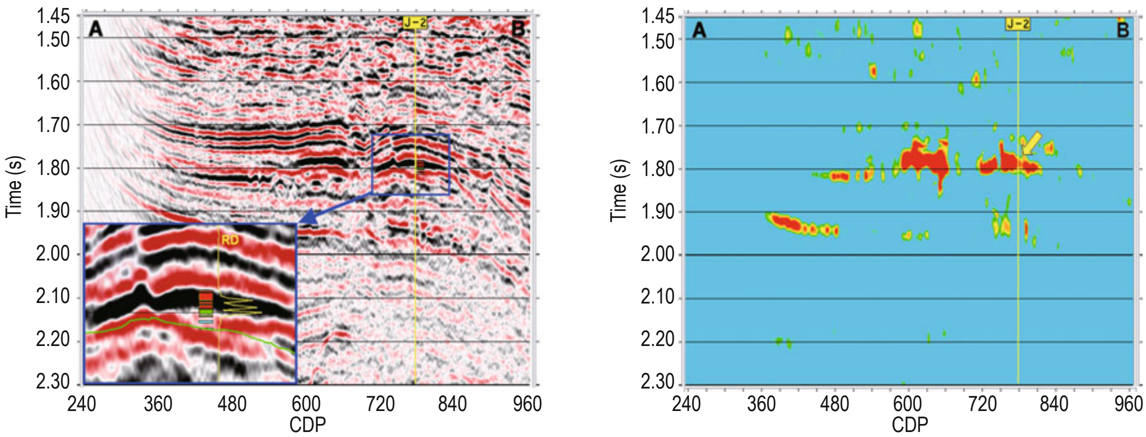

(a) Seismic section (b) Fluid mobility reservoir section

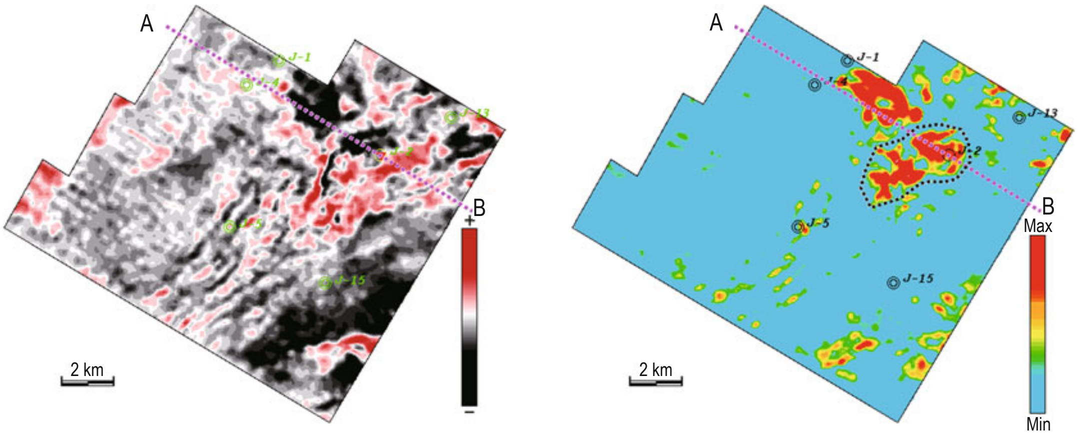

(c) Seismic slice (d) Fluid mobility reservoir slice

Fig. 4 Fluid mobility analysis of reservoirs in the lower Ed2 formation from the JZ area.

(Note that the colors , , and in the well log in the zoomed image indicates gas, oil, and brine, respectively)

Conclusions

Based on the asymptotic analysis of the frequency-dependent reflection coefficient of fluid-saturated reservoirs, we present the implementation methodology of the reservoir fluid mobility measurement calculated from the seismic data. This provides a new means of extracting the permeable reservoir properties and fluid viscosity. Real data examples demonstrate that the reservoir fluid mobility measurement can delineate the location and spatial distribution of productive reservoirs and reduce the uncertainties and ambiguity in fluid identification. The methodology in this paper can be used as a new way to further extract and mine the effective physical properties of reservoirs and fluid signature from seismic data and to expand the value of seismic low-frequency content. It is noteworthy that we can obtain the relative values of the reservoir fluid mobility measurement in the absence of well data. This provides a feasible way to directly predict reservoir accumulations under the circumstance of no drilling. Since the reservoir fluid mobility measurement is extracted from the low-frequency seismic reflection components, it is important to preserve the low-frequency seismic content in data acquisition and processing. Therefore, this can improve the reliability in reservoir fluid mobility extraction based on seismic data.

Acknowledgements

This research was supported by the Cultivating Program of Middle-aged Backbone Teachers of Chengdu University of Technology and the Cultivating Programme of Excellent Innovation Team of Chengdu University of Technology (Grant No. KYTD201002). The authors would like to express their sincere thanks to the anonymous reviewers for their constructive comments and editorial suggestions that significantly improved the quality of the manuscript. We sincerely acknowledge the China National Offshore Oil Corp. (CNOOC) for supplying the marine seismic data. The authors also acknowledge their colleague, Dr. Cai Hanpeng, for his helpful discussion and comments.

References

Batzle, M. L., Han, D., and Hofmann, R., 2006, Fluid mobility and frequency-dependent seismic velocity — Direct measurements: Geophysics, **71**(1), N1 – N9.

Castagna, J. P., Sun, S., and Siegfried, R. W., 2003, Instantaneous spectral analysis: Detection of low-frequency shadows associated with hydrocarbons: The Leading Edge, **22**(2), 120 – 127.

Chen, X., He, Z., He, X., and Hunag, D., 2012, Numeric simulation of frequency-dependent seismic response and hydrocarbon detection, a turbidite reservoir in JZ Area, the Bohai Sea, China: AAPG 2012 Annual Convention and Exhibition, Long Beach, California, USA.

Chen, X. H., He, Z. H., Huang, D. J., and Wen, X. T., 2009, Low frequency shadow detection of gas reservoirs in time-frequency domain: Chinese Journal of Geophysics, **52**(1), 215 – 221.

Chen, X. H., He, Z. H., and Zhong, W. L., 2011, Numeric simulation in the relationship between low frequency shadow and reservoir characteristic: Journal of China University of Mining & Technology, **40**(4), 584 – 591.

Ebrom, D., 2004, The low-frequency gas shadow on seismic sections: The Leading Edge, **23**(8), 772.

Goloshubin, G. M., Connie, V. A., Korneev, V. A., Silin, D., and Vingaov, V., 2006, Reservoir imaging using low frequencies of seismic reflections: The Leading Edge, **25**(5), 527 – 531.

Goloshubin, G. M., Korneev, V. A., and Vingalov, V. M., 2002, Seismic low-frequency effects from oil-saturated reservoir zones: 72th Ann. Internat. Mtg., Soc. Explor. Geophys., Expanded Abstracts, 1813 – 1816.

Goloshubin, G. M., Silin, D., and Vingalov, V., 2008, Reservoir permeability from seismic attribute analysis: The Leading Edge, **27**(3), 376 – 381.

He, Z. H., Xiong, X. J., and Bian, L. E., 2008, Numerical simulation of seismic low-frequency shadows and its application: Applied Geophysics, **5**(4), 301 – 306.

Hilterman, F. J., Patzek, T. W., Goloshubin, G., Silin, D., Sullivan, C., and Korneev, V., 2007, Advanced reservoir imaging using frequency-dependent seismic attributes: http://petroleum.berkeley.edu/patzek/index.htm.

Korneev, V. A., Goloshubin, G. M., Daley, T. M., and Silin, D. B., 2004, Seismic low frequency effects in monitoring fluid-saturated reservoirs: Geophysics, **69**(2), 522 – 532.

Korneev, V. A., Silin, D., Goloshubin, G. M., and Vingalov, V., 2005, Seismic imaging of oil production rate: 75th Ann. Internat. Mtg., Soc. Explor. Geophys., Expanded Abstracts, 1 – 4.

Lichman, E., and Goloshubin, G. M., 2003, Unified approach to gas and fluid detection on instantaneous seismic wavelets: 73th Ann. Internat. Mtg., Soc. Explor. Geophys., Expanded Abstracts, 1699 – 1702.

Lichman, E., Peters, S. W., and Squyres, D. H., 2004a, Wavelet energy absorption-2: Here are velocity aspects of wavelet energy absorption: Oil & Gas Journal, **102**(3), 36 – 44.

Lichman, E., Peters, S. W., and Squyres, D. H., 2004b, Four examples show functions of wavelet energy absorption: Oil & Gas Journal, **102**(4), 48 – 52.

Liu, Y., 2004, Seismic “low frequency shadows” for gas sand reflection: 74th Ann. Internat. Mtg., Soc. Explor. Geophys., Expanded Abstracts, 1563 – 1566.

Quintal, B., Schmalholz, S. M., Podladchikov, Y. Y., and Carcione, J. M., 2007, Seismic low-frequency anomalies in multiple reflections from thinly-layered poroelastic reservoirs: 77th Ann. Internat. Mtg., Soc. Explor. Geophys., Expanded Abst6racts, 1690 – 1695.

Silin, D., and Goloshubin, G. M., 2008, Seismic wave reflection from a permeable layer: Low-frequency asymptotic analysis: ASME 2008 International Mechanical Engineering Congress and Exposition, 47 – 56, Boston, Massachusetts, USA.

Silin, D., and Goloshubin, G. M., 2009, A low-frequency asymptotic model of seismic reflection from a high-permeability layer: Lawrence Berkeley National Laboratory Report, Berkeley, California, USA.

Silin, D., and Goloshubin, G. M., 2010, An asymptotic model of seismic reflection from a permeable layer: Transport in Porous Media, **83**(1), 233 – 256.

Silin, D. B., Korneev, V. A., Goloshubin, G. M., and Patzek, T. W., 2004, A hydrologic view on Biot’s theory of poroelasticity: Lawrence Berkeley National Laboratory Report, Berkeley, California, USA.

Sun, S., Castagna, J. P., and Siegfried, R. W., 2002, Examples of enhanced spectral processing in direct hydrocarbon detection: 72nd AAPG Annual Meeting, Houston, Texas, 10 – 13.

Tai, S., Puryear, C., and Castagna, J. P., 2009, Local frequency as a direct hydrocarbon indicator: 79th Ann. Internat. Mtg., Soc. Explor. Geophys., Expanded Abstracts, 2160 – 2164.

Chen Xue-Hua: See biography and photo in the Applied Geophysics March 2012 issue, P. 72